V. Feliu
Professor,
Department of Ingenieria Electrica.
Electronica Y De Control
E.T.S.I. Industriales De La Uned,
Madrid-28080, Spain

K. S. Rattan
Professor,
Department of Electrical Engineering,
Wright State University,
Dayton, OH 45435

H. B. Brown, Jr.
Robotics Institute,
Carnegie Mellon University,
Pittsburgh, Pennsylvania 15213

Modeling and Control of Single-Link Flexible Arms With Lumped Masses

This paper deals with the modeling and control of a special class of single-link flexible arms. These arms consist of flexible massless structures having some masses concentrated at certain points of the beam. In this paper, the dynamic model of such flexible arms is developed and some of the control properties are deduced. A robust control scheme to remove the effects of friction in the joins is proposed. The control scheme consists of two nested feedback loops, an inner loop to control the position of the motor and an outer loop to control the tip position. The inner loop is described in other publications. A simple feedforward-feedback controller is designed for the outer loop to driw the beam accurately along a desired trajectory. Effects of the changes in the tip's mass are studied. This modeling and control method is then generalized to the distributed-massflexible beam case. Finally, experimental results are presented.

1 Introduction

This paper deals with the modeling and control of a special class of single-link, lumped-mass, flexible arms. These arms consist of massless flexible structures that have masses concentrated at certain points of the beam (see Fig. 1). Although the translations of these masses produce stresses in the flexible structure, their rotations do not generate any torque in the beam. Therefore, the number of vibrational modes in the structure coincides with the number of lumped masses. Book (1979) studied the case of two rigid masses connected by a chain of massless beams having an arbitrary number of rotation joints. Our problem differs from this in the sense that our structure has only one rotation joint and an arbitrary number of lumped masses. These two particular structures are studied because:

- Some lightweight robots and other applications can be reasonably approximated by these models.
- Their dynamics may be easily modeled as compared to distributed-mass flexible arms.
- Interesting properties for the control of flexible arms are deduced from their dynamic models.
- A method to control these arms is inferred from the structure of the model.
- The influence of changes in the tip's mass are easily characterized.
- Given a distributed-mass flexible arm, there always exits a truncated dynamic model which is of the same form as the lumped-mass flexible arm model and which reproduces the dynamics of the measured variables. This allows us to generate the above mentioned control method to the case of distributed-mass flexible arms.

A method to control these flexible arms is proposed in this paper and is based on a robust control scheme developed by Rattan et al. (1988a, 1988b) This method compensates for the effects of Coulomb and dynamic (viscous damping) frictions in the joints. Coulomb friction is a nonlinearity which is typically not taken into account by other methods to control flexible arms. This method proposes the use of two nested feedback loops, an inner loop to control the motor position and an outer loop to control the tip position.

A new method to control the tip position of flexible arms is also proposed in this paper. This method is simpler than the other existing methods but, in turn, needs more sensing. Most methods (Cannon and Schmitz, 1985; Matsuno et al., 1987; Kotnick et al., 1988; etc.) use measurements of the tip and motor variables. This proposed method also uses some sensing at intermediate points of the beam. The number of sensing elements placed on the beam are equal to the number of concentrated masses of the beam. The sensors are located on the masses. Two approaches may be used—sensing positions or

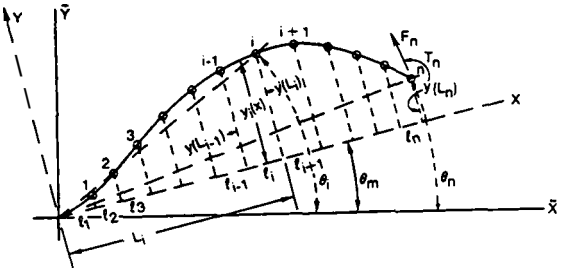

Fig. 1 Lumped masses flexible beam

Contributed by the Dynamic Systems and Control Division for publication in the JOURNAL OF DYNAMIC SYSTEMS, MEASUREMENT, AND CONTROL. Manuscript received by the Dynamic Systems and Control Division March 22, 1989; revised manuscript received March 12, 1991. Associate Editor: S. Jayasuriya.

sensing torques. In the second approach, a sensor is installed at the base of the beam instead of the tip mass. The control scheme developed in this paper is based on position sensing.

Effects of the changes in the carried load on the dynamics of the system are studies. In order to keep the system's response to a reference input approximately constant, the feedforward component of the controller is tuned for a particular payload.

Section 2 establishes the dynamic model of the flexible arms. Some properties that are useful when controlling these arms are deduced in Section 3. The control scheme is proposed in Section 4. Modeling and control methods are extended to the case of distributed mass flexible beams in Section 5. Experimental results are presented in Section 6 and conclusions are drawn in Section 7.

2 Modeling

The model of our flexible arms is divided into two submodels; one describes the behavior of the motor while the other describes the behavior of the mechanical structure using the angle of the motor as its input. These two submodels are coupled by the reaction torque of the beam on the motor (see Fig. 2). This model is quite different from the models normally used in the control of flexible arms that consider the applied torque as the input to the beam (Truckenbrodt, 1979 and Low, 1987). Our representation has an advantage in that it identifies flexible arms with friction in the joints (Feliu et al., 1988), which allows us to compensate for this friction (Rattan et al., 1988b). We show that another advantage of our model is that it allows us to separate the dynamic model terms that depend on the geometry of the beam from the terms that depend on the lumped masses of the beam. Special attention is paid to this issue because this separation of terms will be used in the control design.

2.1 Beam Modeling. Consider the system of Fig. 1. It represents a massless flexible beam with n point masses distributed along the structure with the last mass located at the tip of the beam. The inertia of the motor is included in the motor submodel. Let m_i, $1 \le i \le n$, be the values of the masses; l_i be the distances between consecutive masses $i-1$ and i where l_1 is the distance between the rotation axis of the motor and the first mass. let L_i be the distance between the mass m_i and the axis of the motor. We assume that beam deflections are small enough so that the distances between masses m_i (measured along length of beam) are essentially equal to their projections on the X-axis.

We establish two coordinate systems both with origins at the motor axis. The coordinate system X - Y is fixed in space, whereas the coordinate system X - Y moves with the motor shaft. Thus, y is the distance of a point on the beam from the X-axis. We denote $F(x)$ and $T(x)$ as the force and torque at this point; i.e., the force and torque acting on the beam just to the left of this point due to the action of the beam just to the right of the point.

External forces and torques, F_r, and T_n, applied at the tip of the beam are considered in our model. F_r, represents the component of the resultant applied force that is normal to the beam and to the joint rotation velocity vector simultaneously. T_r, is the component of the resultant torque normal to the X-Y plane. These two terms represents the interaction of the beam with the environment and may be produced by the following: reaction forces when following a surface, the reaction of the next joint when dealing with a multi-link arm, a load, frictional effects on the tip (for example in flexible arms mounted on an air table), etc.

Assuming small deflections, a massless beam can be described by the static deflection relation

$$EI\frac{d^4y}{dx^4}=0$$

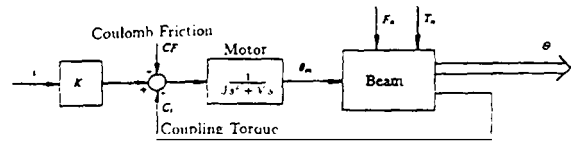

Fig. 2 Dynamic model of the arm

If the stiffness EI is constant through each interval of the beam, the deflection in the interval $[i-1, i]$ is given by a third order polynomial

$$y_i(x)=u_{i,0}+u_{i,1}(x-L_{i-1})+u_{i,2}(x-L_{i-1})^2+u_{i,3}(x-L_{i-1})^3 \tag{1}$$

where $u_{i,j}$ are the polynomial coefficients and are different for each interval, and $L_0 = 0$. We assume in the following analysis that EI is constant throughout the beam. Notice that expression (1) is similar to the equations obtained from finite element models.

2.1.1 Geometric Equations. Imposing continuity conditions between two consecutive intervals up to the second derivative, we get $3(n-1)$ equations

$$\begin{aligned} y_i(L_i)=y_{i+1}(L_i) &\Rightarrow u_{i,0}+u_{i,1}l_i+u_{i,2}l_i^2+u_{i,3}l_i^3=u_{i+1,0}\\ \frac{dy_i}{dx}(L_i)=\frac{dy_{i+1}}{dx}(L_i) &\Rightarrow u_{i,1}+2u_{i,2}l_i+3u_{i,3}l_i^2=u_{i+1,1} \\ \frac{d^2y_i}{dx^2}(L_i)=\frac{d^2y_{i+1}}{dx^2}(L_i) &\Rightarrow u_{i,2}+3u_{i,3}l_i=u_{i+1,2} \end{aligned} \tag{2}$$

for the joint between $[i-1, i]$ and $[i, i+1]$ intervals, where $1 \le i < n$. The continuity condition between the motor and the beam yields

$$y_1(0)=\frac{dy_1}{dx}(0)=0 \Rightarrow u_{1,0}=0,\ u_{1,1}=0, \tag{3}$$

and the condition of the applied torque at the tip gives

$$T_n=EI\frac{d^2y_n}{dx^2}(L_n) \Rightarrow u_{n,2}+3u_{n,3}l_n=\frac{T_n}{2EI} \tag{4}$$

This set of geometrical equations is completed by expressing deflections at specific points i in terms of these polynomials as

$$u_{i,0}+u_{i,1}l_i+u_{i,2}l_i^2+u_{i,3}l_i^3=y(L_i); \quad 1 \le i \le n \tag{5}$$

2.1.2 Dynamic Equations. If we apply Newton's equations to the n masses, we get

$$T(L_i)=\sum_{j=i+1}^{n} m_j(L_j-L_i)\frac{d^2\hat{y}(L_j)}{dt^2} - T_n - F_n(L_n-L_i) \quad 0 \le i < n \tag{6}$$

$$F(L_i)=-\sum_{j=i+1}^{n} m_j\frac{d^2\hat{y}(L_j)}{dt^2}+F_n \quad 0 \le i < n \tag{7}$$

where $\hat{y}(L_j) = y(L_j)+\theta_m L_j$ is the arc position of mass j with respect to the origin axis (θ_m is the angle of the motor). Taking into account that

$$u_{i,2}=\frac{T(L_{i-1})}{2EI}, \quad u_{i,3}=-\frac{F(L_{i-1})}{6EI} \tag{8}$$

and combining (6)-(8), we get

$$\frac{d^2\hat{y}(L_i)}{dt^2}=\frac{6EI}{m_i}(u_{i,3}-u_{i+1,3}); \quad 1 \le i \le n \tag{9}$$

where $u_{n+1,3} = -F_n/6EI$ is defined according to (8). Expression (9) is obtained from (7) using the second equation of (8). An equivalent expression may be obtained from (6) since expressions (2)–(8) are not independent. But we used (7) because the resulting expression is simpler.

2.1.3 Dynamic Model of the Beam. Equations (2)–(5) allow us to express coefficients $u_{i,j}$ as linear functions of $y(L_i)$ and $T_{,,}$. The $u_{i,3}$ coefficients can be expressed in compact form as

$$\begin{pmatrix} u_{1,3} \\ u_{2,3} \\ \vdots \\ u_{n,3} \end{pmatrix} = \mathbf{u} \begin{pmatrix} y(L_1) \\ y(L_2) \\ \vdots \\ y(L_n) \\ T_n \end{pmatrix} \tag{10}$$

where $\mathbf{u}$ is a constant matrix that depends only on the dimensions of the beam and the location of the masses. Denoting θ_i as the angle between the X-axis and the radial line from the origin to mass i (see Fig. 1), using the approximation $\theta_i = \hat{y}(L_i)/L_i$, and substituting (10) into (9), we get n linear equations of the form

$$\frac{m_i}{EI}\frac{d^2\theta_i}{dt^2} = \sum_{j=1}^{n} a_{i,j}\theta_j + b_i\theta_m + \frac{p_i}{EI} T_{,,}; \quad 1 \le i < n \tag{11}$$

$$\frac{m_n}{EI}\frac{d^2\theta_n}{dt^2} = \sum_{j=1}^{n} a_{n,j}\theta_j + b_n\theta_m + \frac{p_n}{EI} T_n + \frac{1}{L_n EI} F_n. \tag{12}$$

Equations (11) and (12) can be expressed in compact form as

$$\mathrm{M}\frac{d^2\Theta}{dt^2} = EI[\mathbf{A}\theta + \mathbf{B}\theta_m] + \mathbf{P}T_{,,} + \mathbf{Q}F_n \tag{13}$$

where $\mathrm{M} = \mathrm{diag}(m_1, m_2, \ldots, m_n)$, $\Theta^T = (\theta_1, \theta_2, \ldots, \theta_n)$. A is an n x n constant matrix, and $\mathbf{B}$, $\mathbf{P}$ and $\mathbf{Q}$ are constant n x 1 column vectors. In particular $Q^T = (0, 0, \ldots, 0, L_n^{-1})$. In expression (13), A, $\mathbf{B}$, $\mathbf{P}$ and $\mathbf{Q}$ depend only on the geometry of the beam. The values of the lumped masses influence only matrix M.

2.2 Motor Modeling. The dynamic behavior of a dc motor may be modeled as

$$Ki = J\frac{d^2\theta_m}{dt^2} + V\frac{d\theta_m}{dt} + C_t + CF \tag{14}$$

where K is the electromechanical constant of the motor, i is the current, J is the polar inertia of the motor, V is the dynamic friction coefficient, C_t is the coupling torque between motor and beam and CF is the Coulomb friction. Taking into account that $C_t = -T(0) = -2EIu_{1,2}$, we can express this torque as a linear function

$$C_t = \mathbf{H}\Theta + h_{n+1}\theta_m + h_{n+2}T_n, \tag{15}$$

where $\mathbf{H} = (h_1, h_2, \ldots, h_n)$; h_i, $1 \le i \le n+2$ are parameters that do not depend on the masses of the beam.

Expressions (13)–(15) suggest an easy way of extending this method of modeling to multi link arms. Expression (13) is obtained for each link, and expressions (14) and (15) for each joint. The coupling between each pair of links is obtained by making the $T_{,,}$ of the ith link equal to the C_t of the $(i+1)$st link.

3 Properties of the Lumped-Mass Model

The dynamics of the flexible arm as described by Eqs. (13)-(15) are represented in Fig. 2. We assume that F_n and T_n are perturbations in the system. In order to perform the analysis and design of the control system, we make $F_n = T_{,,} = 0$. Five interesting properties from the control point of view are given below.

1. From (13) and using Laplace transforms, we find that the transfer functions $G_i(s) = \theta_i(s)/\theta_m(s)$, for $1 \le i \le n$, have terms only of the form s^{2j}; $0 \le j \le n$, n being the number of lumped masses. Poles and zeros always come from factors of the form: $(s^2 + z)$, with z generally being a complex number. The following cases are possible:

(a) $z \in \mathbb{R}, z > 0 \Rightarrow$ two conjugate roots on the imaginary axis.

(b) $z \in \mathbb{R}, z < 0 \Rightarrow$ two roots on the real axis, being of the same magnitude but opposite sign.

(c) $z \in \mathbb{C}, F(z) \neq 0 \Rightarrow$ sets of four symmetrical roots with respect to both real and imaginary axes.

The mechanical structure is marginally stable because we assume that there is no friction along the beam (no energy dissipating phenomena) and the friction on the tip is treated as a perturbation. The poles are always of class (a), but the zeros may be of any of the three classes. Case (b) appears quite often and produces nonminimum phase systems. Control of these systems presents some difficulties as stated in Cannon and Schmitz (1985).

2. The difference between the orders of the denominator and numerator of $G_i(s)$, $\forall i$, is at least two. This is a consequence of dealing with flexible arms. If numerator and denominator were of the same order, it would mean that an instantaneous change in the position of the motor would produce an instantaneous change in the position of the ith point of the flexible arm (*Initial Value Theorem* of Laplace transforms, see Kuo (1982), which is not possible because flexible beams need some time to propagate the motion along the structure.

3. ***Separation Property.*** It was mentioned in the previous section that the influence of the lumped masses on the dynamics of the arm may be perfectly seprated from the influence of the geometrical dimensions of the beam (see Eqs. (13) and (15)). This occurs because the beam is modeled as massless; thus, its shape is given by static deflection equations that depend only on the position coordinates. This property is used in the controller design.

4. Zeros *Invariance Property.* Zeros of $G_{,,}(s)$, the transfer function between the tip position θ_n and the angle of the motor θ_m, remain constant and are independent of the payload of the tip.

5. The coupling torque C_t does not depend explicitly on the external force, $F_{,,}$ applied at the tip (see (15)). This is because the force applied to the tip does not appear in the geometric equations.

These properties are also verified for distributed-mass flexible arms and will be used in the next section.

4 Control Method

To control our flexible arms, a scheme based on two nested feedback loops is proposed. An inner loop is used to control the position of the motor and an outer loop is used to control the tip position (see Fig. 3). The controller of this outer loop generates a control signal which is the reference for the position of the motor (θ_{mr}) in the inner loop. This scheme was shown to be robust in the sense that it minimizes the effects of the Coulomb friction in the control as well as the effects of unexpected changes in the dynamic friction (Rattan et al. 1988a).

Details of the design of the inner loop may be found in Rattan et al. (1988c). Because the motor is a minimum phase system, the inner loop uses very high feedback gains relative to the gain of the outer loop. The inner loop also incorporates compensation terms for the Coulomb friction and the coupling torque between the motor and the beam (see Fig. 4). The compensation term for the motor-beam coupling may be easily implemented in our arms using (15). Because of these high gains, the positioning of the motor can be made substantially faster than the dynamics of the vibration modes of the beam. If the positioning of the motor is much faster than the dynamics of the beam, the dynamics of the inner loop can be neglected ($\theta_m = \theta_{mr}$), and the design of the tip position control loop is significantly simplified. We assume, in what follows, that $\theta_m = \theta_{mr}$, and also that $T_{,,} = F_{,,} = 0$.

The controller for the tip position is composed of a combined feedforward/feedback law (Fig. 5). The feedforward com-

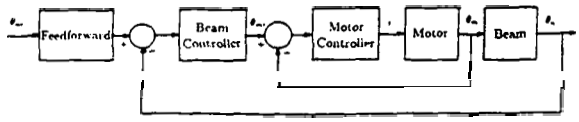

fig. 3 Control scheme robust to friction

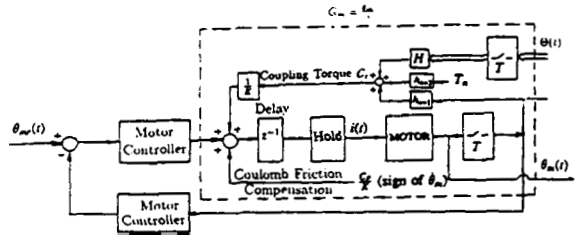

Fig. 4 Computer control loop of the motor position

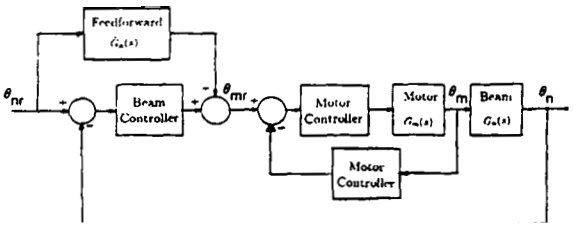

Fig. 5 Proposed tip position controller

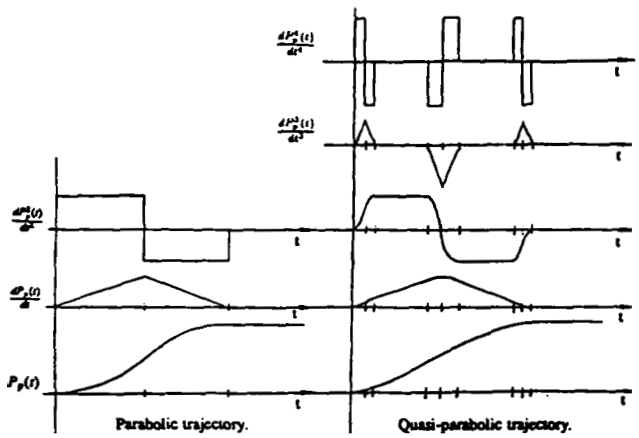

Fig. 6 Nominal trajectories for the tip position (P_p).

ponent is responsible for driving the tip of the arm close to the desired trajectory and the feedback term is responsible for correcting tracking errors. Both components are designed considering that the input of the system is the desired angle of the motor θ_{mr}.

4.1 Feedforward Term. If the transfer function between the angle of the motor and the angle of the tip $G_n(s)$ is minimum phase, then a second order parabolic profile can be used and the feedforward term can be $G_n^{-1}(s)$. But if this transfer function is non-minimum phase, then a quasi-parabolic profile with derivatives bounded up to the fourth order (see Fig. 6) is used in order to guarantee the implementability of the feedfoward term (Feliu et al., 1988) and the nominal quasi-parabolic profile is passed through a special filter in order to avoid unbounded control signals. We denote that nominal trajectory as P_p.

The necessity of the above mentioned filter may be justified

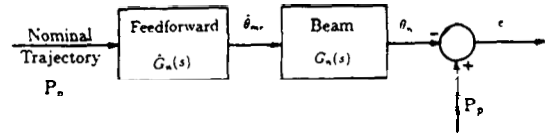

Fig. 7 Feedforward control

from Fig. 7. Assume an open-loop control for the case without external perturbations. If we want the tip to follow the reference exactly, then the control signal $\hat{\theta}_{mr}$ (which is same as θ_m neglecting the dynamics of the inner loop) is obtained by passing the desired profile P_p through a block $G_n(s)$ that implements the inverse of the plant $G_n(s)$. If this plant had zeros in the right half-plane, they would become unstable poles in $G_n^{-1}(s)$ producing an unbounded $\hat{\theta}_{mr}$ control signal. In order to avoid this, a modified $\hat{G}_n(s)$ term must be used and the tip reference would now be given by

$$\theta_{nr}(s) = G_n(s)\hat{G}_n(s)P_p(s), \tag{16}$$

where $P_p(s)$ is the Laplace transform of the parabolic or quasi-parabolic profile. This filter is chosen in such a way to get a reference trajectory θ_{nr} as close as possible to the desired reference P_p, taking into account the constraint of a bounded $\hat{\theta}_{mr}$. We choose as a representative index of closeness between trajectories, the integral of the squared difference between both profiles (see Fig. 7). This can be written as

$$J = \int_0^\infty e^2(t)dt = \frac{1}{2\pi j}\int_{-j\infty}^{j\infty} \frac{2}{s^3} \times (1 - G_n(s)\hat{G}_n(s))\,\frac{2}{-s^3}\,(1 - G_n(-s)\hat{G}_n(-s))ds, \tag{17}$$

where a parabolic profile $2/s^3$ has been assumed for P_p because, from Fig. 6, the quasi-parabolic profile behaves as a parabolic trajectory most of the time, becoming a fourth order parabola only during the short transitions from maximum to minimum acceleration and vice versa. The transfer function $G_c(s)$ that minimizes (17) is a Weiner filter and gives a better performance than any simple feedback controller, provided there are no perturbations in the system. A feedback version of the Wiener filter also exists, but it gives complex controllers that are difficult to implement in a real-time control. An advantage of a feedforward controller is that if we know the reference trajectory, the feedforward signal can be computed off-line in advance of the motion. Assuming that $G_n(s)$ is of the form

$$G_n(s) = K\,\frac{\prod_{i=1}^{n_1}(s-a_i)\prod_{j=1}^{n_2}(s-b_j)}{D(s)},$$

where $a_i < 0$, $1 \le i \le n_1$; $b_j > 0$, $1 \le j < n_2$, and all the roots of $D(s)$ are in the left half-plane of the s-plane. It can be shown (Gupta and Hasdorff, 1970 and Feliu et al., 1989) that the optimum $\hat{G}_n(s)$ that minimizes the cost defined in (17) is given by

$$\hat{G}_n(s) = \frac{D(s)(\alpha_2 s^2 + \alpha_1 s + \alpha_0)}{K\prod_{i=1}^{n_1}(s-a_i)\prod_{j=1}^{n_2}(s+b_j)} \tag{18}$$

where the coefficients α's are obtained from the partial fraction expansion of $\dfrac{\prod_{j=1}^{n_2}(s+b_j)}{s^3\cdot\prod_{j=1}^{n_2}(s-b_j)}$, α_0, α_1, α_2 being the coefficients corresponding to the terms whose denominators are s, s^2, s^3, respectively. The filter is then written as

$$G_n(s)\hat{G}_n(s) = (\alpha_2 s^2 + \alpha_1 s + \alpha_0)\frac{\prod_{j=1}^{n_2}(s-b_j)}{\prod_{j=1}^{n_2}(s+b_j)}. \quad (19)$$

4.2 Feedback Term. Feedback controllers may be designed by using any of the standard control design methods. Good results are achieved by using optimization techniques (Lee and Markus, 1986) to design the controller: $\gamma(s) = -\Lambda x(s)$, that drives x from an initial state to the zero state minimizing a cost function of the form

$$J = \int_{t=0}^{\infty} (x^T(t) Q_1 x(t) + Q_2 \theta_{mr}^2(t))dt \quad (20)$$

where $Q_1 \in \mathbb{R}^{2n\times 2n}$, $Q_2 \in \mathbb{R}$ are weighting matrices and $x \in \mathbb{R}^{2n}$ is the state vector of the system. From *(13)* and making $T_n = Q_n = 0$, we get the state equation of the system

$$\dot{x}(t) = \underbrace{\begin{pmatrix} 0 & I_n \\ EIM^{-1}A & 0 \end{pmatrix}}_{A} x(t) + \begin{pmatrix} 0 \\ EIM^{-1}B \end{pmatrix}\theta_m(t) \quad (21)$$

where $x^T(t) = (\Theta^T \dot{\Theta}^T)$ and $I_n \in \mathbb{R}^{n\times n}$ is the identity matrix. Model *(21)* is simpler than the models used in other approaches which relate $\theta_n(t)$ and $\theta_m(t)$ with motor current $i(t)$. This is because it does not include motor dynamics (motor inertia and the coupling term) which have been approximately cancelled by the motor control loop. This allows the design of simple controllers for the tip position. If there were dynamic friction in the tip, then F_r would be proportional to the speed of the tip mass and a coefficient would appear in the $(2n, 2n)$ position of matrix A of equation *(21)*.

This feedback scheme uses the errors between the desired and the actual states to generate the control signal. Defining $\Lambda = (\Lambda_1\ \Lambda_2);\ \Lambda_1, \Lambda_2 \in \mathbb{R}^{1\times n}$ we can express the control signal, γ, as a function of the measured variables as $\gamma(s) = (\Lambda_1 + \Lambda_2 s)(\Theta_r(s) - \Theta(s))$. The reference vector for the measured variables (Θ_r) may be obtained from the reference θ_{nr} by using the following expression

$$\Theta_r(s) = \Upsilon(s)\theta_{nr}, \quad (22)$$

where

$$\Upsilon(s) = \begin{pmatrix} C_1 Adj(Ms^2 - EIA)EIB \\ C_2 Adj(Ms^2 - EIA)EIB \\ \vdots \\ C_n Adj(Ms^2 - EIA)EIB \end{pmatrix} \frac{1}{C_n Adj(Ms^2 - EIA)EIB} \quad (23)$$

where $C_i = (0 \ldots 0\ 1\ 0 \ldots 0)$, the 1 being in the ith column. In the case of a non-minimum phase system, the denominator of expression (23) has some positive real component roots. However, they are cancelled with the zeros of filter (19), leaving $\theta_r(t)$ bounded. Cancellation may be exactly done because all these terms are computed.

The feedback control scheme proposed in this paper presents advantages over the other existing schemes that use less sensors when implementing it on a digital computer. These other control schemes need to reconstruct the states x from the measurements of the motor and tip of the arm by means of filters and observers. They involve a large amount of computation. Also, in many cases, these reconstructions are distorted by the noise of the measured signals requiring some filtering of the measurements. This requires more complex algorithms (Kalman filters, etc.) and more computations. But in our case, because we have simplified the ann dynamics by closing the motor position loop and since we are using more sensing in the beam, all the states may be obtained easily. Positions are measured and velocities may be estimated from measurements

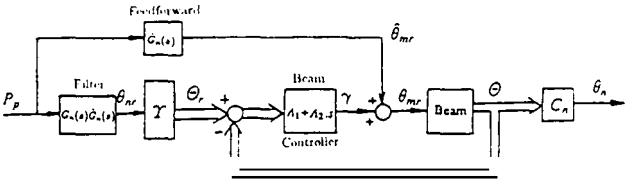

Fig. 8 Detailed scheme of the tip position controller

by using algorithms that are simpler than the one needed to estimate states in methods that use less sensing. In fact, in our experiments, where the level of noise was about 1 mrad for a range of motion of about *200* mrad, a good estimate of the velocity was obtained by using the simple difference equation $\dot{\Theta}(kT) = (\Theta(kT) - \Theta((K-1)T))/T$, where T is the sampling period and k is an integer. Because only the first derivative of measured signals is needed, this approximation of the velocities of the mass points is reasonable in many cases.

Figure 8 shows the details of this control scheme. Notice that the first derivatives of the position error signals are used instead of the first derivatives of the position states.

4.3 Influence **of the Payload.** In this subsection, effects of changes in the payload on the dynamics of the controlled system are studied.

4.3.1 Inner **Loop.** The motor position control loop is not directly affected by changes in the payload. The payload influences the dynamics of this loop only through the coupling torque between the motor and the beam. This coupling is being compensated by the term (15) that estimates coupling torque from position measurements. Coefficients h_i are independent of the payload and consequently no term of the inner loop needs to be tuned as a function of the payload.

The payload affects this loop indirectly, if we consider the saturation limits of the motor current. If the payload is too high, the current saturates and control performance deteriorates. However, for the normal range of payloads, performance of this inner loop may be considered invariant.

4.3.2 Feedforward Term. Because of *Zero Invariancy Property*, the filter expressed in (19) is independent of the load and variations in the feedforward term (18) are due only to the factor $D(s)/K$. Therefore, $\hat{G}_n(s)$ can be easily tuned to payload changes by changing only one parameter in its numerator as will be illustrated in the example.

4.3.3 Feedback Term. The gain factor and poles of the closed-looptransfer functions matrix $G(\Theta_N(s) = G(s)\Theta_{nr}(s))$ change with the payload. However, zeros of the transfer functions $G_{n,i}$; $1 < i \le n$ of the last row of this matrix remain constant. Notice that these transfer functions characterize the closed-loop dynamic behavior of the tip of the arm.

Finally, only the numerators of T are affected by the changes in the payload. Their dependence on m_n is similar to the dependence of $\hat{G}_n(s)$.

The control scheme (based on two nested feedback loops) described in this paper can be extended to multi-link flexible arms. Multi linke arms generally are multivariable and nonlinear systems. Techniques used for the multi-link rigid arms (Craig, 1986) may be combined with this scheme to control multi-link flexible arms. In this case, the proposed feedforward term can not be used, but the two nested feedback loop schemes seems to be effective in controlling multi-link flexible arms with Coulomb friction in the joints. In fact, a first results is presented in Feliu et al. (1989), where a two degrees of freedom lightweight flexible manipulator is modeled and controlled using the technique described in this paper.

5 Generalization to Distributed Mass Flexible Arms

This section extends the proposed modeling method to the

case of flexible arms with distributed masses. The following lemma is proposed.

Lemma: Let us assume that

1. There are no internal energy dissipating phenomena in the structure of a distributed mass flexible arm. Energy dissipation happens only in the joint (from friction). This means that property 1 of Section 3 remains true here. Property 2 is also true because the motion propagation from the base to the tip of the sturcture is not instantaneous.

2. State-space model of the distributed mass flexible arm may be truncated keeping in the model just the first and few representative vibrational modes and neglecting the other high frequency modes. This truncation is typically performed as a preliminary step in the design of controllers for flexible arms.

3. We measure the position at n points of the beam. We choose n equal to the number of vibrational modes considered in the truncated model of the beam, N_v.

Then a truncated model of the same form as lumped-mass flexible beam models

$$\frac{d^2\Theta}{dt^2} = \quad + g\mathbf{e}_m \tag{24}$$

$$C_t = \bar{\mathbf{H}}\Theta + \bar{h}_{n+1}\theta_m \tag{25}$$

can be defined that reproduces the dynamics of the distributed mass flexible beam for the range of frequencies of interest.

This model represents the truncated dynamics of the distributed mass flexible beam. External perturbations T_p and F_p were assumed to be 0 when deriving this model. Notice now that $\bar{\mathbf{A}}$, $\bar{\mathbf{B}}$ depend on the distributed mass of the beam. The following procedure is proposed to obtain this model from experimental measurements on a distributed-mass system.

Procedure

1. Experimentally obtain the frequency response between the angle of the motor and the angle of the tip.

2. Fit a tansfer function $\bar{G}_t(s)$, that relates the angle of the tip with the angle of the motor, to this frequency data. This transfer function must exhibit properties 1 and 2 of Section 3. The order of the denominator divided by two is the number of vibrational models. N_v, considered in the model.

3. Experimentally obtain the frequency responses, with respect to the angle of the motor, of other $N_v - 1$ points of the structure. No special conditions about the location of these points is required a priori. The only constraint to consider when choosing the $N_v - 1$ sensed points is that the numerators μ_i of the identified transfer functions at the N_v points should be linearly independent to permit inversion of the matrix that appears in (29). This means that very close points cannot be used for sensing. The position at the intermediate points of the beam can be obtained by placing LED's at the desired points and using a camera that simultaneously tracks them. In our experiments, we used a Selspot tacking camera to obtained the positions at the intermediate points.

4. Identify other $N_v - 1$ transfer functions $\bar{G}_i(s)$ from this data. The poles are common to all of the systems so these transfer functions will have the same denominator as $\bar{G}_t(s)$.

5. Model (24) may be obtained from these identified transfer functions $\bar{G}_1$, $\bar{G}_2$, $\bar{G}_3$, . . . , $\bar{G}_{Nv-1}$, $\bar{G}_{Nv}$ (we denote $\bar{G}_{Nv}$ as $\bar{G}_{Nv}$) with the following procedure:

Let $\Theta \in \mathbb{R}^{N_v \times 1}$ is the column vector that represents the measured angles $\theta_1, \theta_2, \ldots, \theta_N$, at the selected points of the structure;

$$\bar{G}_i(s) = \frac{(\mu_i\ 0)\mathbf{S}}{\delta\mathbf{S}}, \quad 1 \le i \le N_v \tag{26}$$

where $\mathbf{S}^T = (1\ s^2\ s^4\ \ldots\ s^{2N_v})$, $\mathbf{S} \in \mathbb{R}^{N_v+1}$;

$$\mu_i = (\mu_{i,0}\ \mu_{i,1}\ \mu_{i,2}\ \ldots\ \mu_{i,N_v-1}), \quad \mu_i \in \mathbb{R}^{N_v};$$

$$\delta = (\delta_0\ \delta_1\ \delta_2\ \ldots\ \delta_{N_v-1}\ 1), \quad \delta \in \mathbb{R}^{N_v+1}.$$

Notice that $\bar{G}_i$ is of this form because of properties 1 and 2 of Section 3, then

$$\frac{d^2\theta_i}{dt^2} = s^2\,\frac{(\mu_i\ 0)\mathbf{S}}{\delta\mathbf{S}}\,\theta_m(s) = \frac{(0\ \mu_i)\mathbf{S}}{\delta\mathbf{S}}\,\theta_m(s). \tag{27}$$

If $\bar{a}_{i,j}$ are the elements of $\bar{\mathbf{A}}$ and $\bar{b}_i$ the elements of column Bin Eq. (24), then substituting (26)–(27) in (24) and identifying coefficients in the numerator, we get

$$(0\ \mu_i) = \sum_{j=1}^{N_v} \bar{a}_{i,j}(\mu_i\ 0) + \bar{b}_i\delta$$

and the coefficients of model (24) are obtained from

$$\bar{\mathbf{B}}^T = (\mu_{1,N_v-1}, \mu_{2,N_v-1}, \ldots, \mu_{N_v,\,N_v-1}) \tag{28}$$

$$\bar{\mathbf{A}} = \begin{pmatrix} \lambda_1 \\ \lambda_2 \\ \lambda_3 \\ \vdots \\ \lambda_{N_v} \end{pmatrix} \begin{pmatrix} \mu_1 \\ \mu_2 \\ \mu_3 \\ \vdots \\ \mu_{N_v} \end{pmatrix}^{-1} \tag{29}$$

where rows $\lambda_i \in \mathbb{R}^{1 \times N_v}$ are calculated from

$$(0\ \mu_i) - \mu_{i,N_v-1}\delta = (\lambda_i\ 0). \tag{30}$$

6. Expression (25) for the motor-beam coupling torque C_t may be obtained by using the procedure

(a) Identification of the linear part of the dynamics of the motor, transfer function $\bar{G}_m(s) = \theta_m(s)/i(s)$.

(b) Distortions in the identification because of the Coulomb friction may be avoided by using the procedure described in Feliu et al. (1988).

(c) Denoting $C_t(s) = (N_c(s)/D_c(s))\,\theta_m(s)$ and substituting in (14) (after making $C_F = 0$), we get

$$KD_c(s)\bar{G}_m^{-1}(s) = (Js^2 + Vs)D_c(s) + N_c(s).$$

Equation (15) expresses C_t as a linear combination of the positions of the masses and the motor. Then, the transfer function $C_t(s)/\theta_m(s)$ will have the same poles as transfer function $G_i(s) = \theta_t(s)/\theta_m(s)$ and therefore its denominator, $D_c(s)$, is given by $\delta\mathbf{S}$. Substituting $D_c(s) = \delta\mathbf{S}$ in the above motor dynamics equation, we can obtain motor inertia J, friction V and $N_c(s)$. K is obtained from the manufacturer's specifications.

(d) (25) is obtained from polynomials N_c and D_c following an algebraic process similar to that shown in step 5 of the procedure for obtaining this model.

The model given by Eqs. (24)–(25) allows us to use the method of Section 4 to control distributed-mass flexible arms with complete generality. Given a model (24)–(25), it is possible to build an equivalent lumped-mass flexible arm that exhibits these dynamics. It can be easily seen that this can be done exactly only when $N_v = 1$. But for higher N_v, lumped-mass flexible arms that approximately reproduced the dynamics (24)–(25) can be found.

A consequence of this last paragraph is that: it it not necessary to build distributed-mass flexible arms in order to test control schemes for flexible arms. Lumped-mass flexible arms (which may be easier to build, model and identify) may be used in many cases as prototype of real flexible arms, allowing us to test control laws on them before implementation on real arms.

6 Experimental Results

Modeling and control methods described in this paper are applied here to a single-link flexible arm with lumped masses that has been built in our laboratory. It is composed of two lumped masses, yielding a non-minimum phase system.

6.1 Experimental Setup. The mechanical system consists

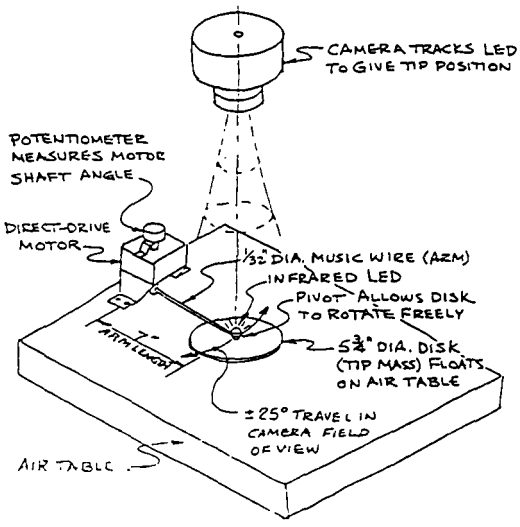

Fig. 9 Experimental setup

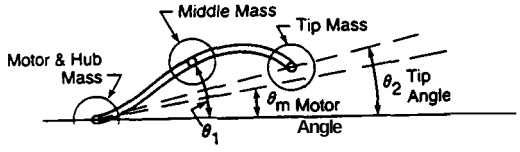

Fig, 10 Two-mass flexible beam

of a dc motor, a slender arm attached to the motor hub and two masses floating on an air table. One mass is attached at the middle of the arm and the other at the tip of the beam. Figure 9 shows the major parts of the system and Fig. 10 shows the arrangement of this two-mass beam. The arm is a piece of music wire (12 in long and 0.047 in. in diameter) clamped in the motor hub. Bothmassesare 1/16 in. thick, 5 3/4 in diameter fiberglass disks attached at their centers to the middle and end of the beam with freely pivoted pin joints. These disks have masses of 0.119 lb and float on the horizontal air table with minimal friction. Because the mass of the beam is small compared to that of these disks, and because the pinned joints prevent generation of torques at the middle and end of the beam. this mechanical system behaves practically like an ideal, two-Iumped-mass flexible arm.

An Inland direct-drive motor drives the arm. Amplifier current limit is set to 4.12 amp. which corresponds to 9.0 lb in. motor torque. Coulomb friction of the motor is about .288 in. (corresponding to .132 amp) and has a significant effect on the control when the torque to the arm is low, as with our very slender arm.

Two sensors are used for the control of the system. A 7/8 in., 360 degrees of potentiometer provides the angle of the motor shaft. A Selspot tracking camera is used that simultaneously sensesthe X-Y positions of two infrared LED mounted on the two masses of the arm.

The control algorithm is implemented on a Omnibyte OB68K1A, MC 68000 based computer with 512K bytes dynamic RAM and 10MHZ clock. Because the control computer is relatively slow. real computations are done in integer or short integer mode. Analog interfacing is provided with 12bit A/D and D/A boards. The sampling period used to control both arms in 3 ms.

6.2 Modeling. In this subsection, the dynamic equations of the two-mass beam and the coupling between motor and beam are developed using the method of Section 2. Parameters of the motor submodeled are also given. They can be obtained from the identification method described in Feliu et al. (1988). The procedure of Section 2 is

Geometric equations:

- Equations (2):

$$u_{1,0}+u_{1,1}l_1+u_{1,2}l_1^2+u_{1,3}l_1^3=u_{2,0}$$
$$u_{1,1}+2u_{1,2}l_1+3u_{1,3}l_1^2=u_{2,1}$$
$$u_{1,2}+3u_{1,3}l_1=u_{2,2}$$

- Equation (3): $u_{1,0}=u_{1,1}=0$.
- Equation (4): $u_{1,2}+3l_1u_{1,3}=\dfrac{T_2}{2EI}$.
- Equations (5):

$$u_{1,0}+l_1u_{1,1}+l_1^2u_{1,2}+l_1^3u_{1,3}=y(l_1)$$
$$u_{2,0}+l_2u_{2,1}+l_2^2u_{2,2}+l_2^3u_{2,3}=y(l_1+l_2)$$

Dynamic equations:

- Equations (9):

$$l_1\frac{de,}{dt^2}=\frac{6EI}{m_1}(u_{1,3}-u_{2,3})$$

$$(l_1+l_2)\frac{d^2\theta_2}{dt^2}=\frac{6EI}{m_2}\left(u_{2,3}+\frac{F_2}{6EI}\right)$$

Dynamic model of the beam:

- Equation (10):

$$\begin{bmatrix}u_{1,3}\\u_{2,3}\end{bmatrix}=\mathfrak{U}\begin{bmatrix}y_1\\y_2\\T_2\end{bmatrix} \tag{31}$$

where

$$\mathfrak{U}=\frac{1}{l_1l_2(3l_1+4l_2)}\begin{bmatrix}\dfrac{-3l_1^2+6l_1l_2+2l_2^2}{l_1^2} & 3 & -\dfrac{l_2^2}{2EI}\\ \dfrac{2l_1+3l_2}{l_2} & -\dfrac{2l_1}{l_2} & \dfrac{l_1(l_1+2l_2)}{2EI}\end{bmatrix}.$$

- Substituting in the above equation $y_1=l_1(\theta_1-\theta_m)$, $y_2=(l_1+l_2)(\theta_2-\theta_m)$, and combining it with the dynamic equations, we obtain from Eq. (13)

$$\mathfrak{M}\begin{bmatrix}\dfrac{d^2\theta_1}{dt^2}\\ \dfrac{d^2\theta_2}{dt^2}\end{bmatrix}=EI(\mathfrak{A}\begin{bmatrix}\theta_1\\\theta_2\end{bmatrix}+\mathfrak{B}\theta_m)+\mathfrak{P}T_2+\mathfrak{Q}F_2 \tag{32}$$

where

$$\mathfrak{M}=\begin{bmatrix}m_1 & 0\\0 & m_2\end{bmatrix},\quad \mathfrak{P}=\begin{bmatrix}-\dfrac{l_1+l_2)^2}{2EI}\\ \dfrac{l_1(l_1+2l_2)}{2EI}\end{bmatrix},\quad \mathfrak{Q}=\begin{bmatrix}0\\ \dfrac{1}{l_1+l_2}\end{bmatrix},$$

$$\mathfrak{A}=\frac{6}{l_1^2l_2(3l_1+4l_2)}\begin{bmatrix}-\left(6l_1+6l_2+2\dfrac{l_2^2}{l_1}+2\dfrac{l_1^2}{l_2} & (l_1+l_2)\left(3+2\dfrac{l_1}{l_2}\right)\right.\\ (2l_1+3l_2)\dfrac{l_1}{l_2} & (-2(l_1+l_2)\dfrac{l_1}{l_2}\end{bmatrix},$$

$$\text{and } \mathfrak{B}=\frac{6}{l_1^2l_2(3l_1+4l_2)}\begin{bmatrix}l_1+3l_2+2\dfrac{l_2^2}{l_1}\\ -l_1\end{bmatrix}.$$

Coupling torque (15):

$$C_2 = -2EIu_{1,2} = 2EIl_1u_{1,3} - \frac{2EIy_1}{l_1^2}$$

$$= \mathcal{K}\begin{bmatrix}\theta_1\\ \theta_2\end{bmatrix} + \frac{12EI(l_1+l_2)}{l_1(3l_1+4l_2)}\theta_m - \frac{l_2}{(3l_1+4l_2)}T_2, \quad (33)$$

where

$$\mathcal{K} = \frac{6EI(l_1+l_2)}{l_2(3l_1+4l_2)}\begin{bmatrix} -\left(1+2\frac{l_2}{l_1}\right) & 1\end{bmatrix}.$$

Substituting the mechanical parameters: E = **30** x 10^6 lb/in.^{2}, Z = $0.047^4/64\ \pi$ in.^{4}, $m_1 = m_2 =$ **0.121** lb and $l_1 = l_2$ = **6** in. in Eqs. **(32)** and **(33),** we get

$$\mathfrak{M} = \begin{bmatrix}0.12136 & 0\\ 0 & 0.121361\end{bmatrix}, \quad \mathfrak{A} = \begin{bmatrix}-176.6032 & 110.377\\ 27.59425 & -22.0754\end{bmatrix}, \quad \mathfrak{B} = \begin{bmatrix}66.2262\\ -5.51885\end{bmatrix},$$

$$\mathcal{P} = \begin{bmatrix}-0.047619\\ 0.017857\end{bmatrix}, \quad \mathcal{Q} = \begin{bmatrix}0\\ 0.0833\end{bmatrix}, \quad \mathcal{K} = \begin{bmatrix}-6.159\\ 2.053\end{bmatrix}, \quad h_3 = 4.106 \text{ and } h_4 = -0.1429.$$

Assuming $T_2 = F_2 = 0$, we obtain (from **(32))** the following transfer functions

$$\frac{\theta_1(s)}{\theta_m(s)} = \frac{545.7(s^2+106.1)}{s^4+1637.1s^2+57903.3} \quad (34)$$

$$\frac{\theta_2(s)}{\theta_m(s)} = \frac{-45.5(s^2-1273.3)}{s^4+1637.1s^2+57903.3} \quad (35)$$

Theoretical natural frequencies of the beam were obtained from the poles of the above transfer functions. They are **6.014** rad/s **(0.957 Hz)** and **40.0116** rad/s **(6.368 Hz).** These frequencies were later measured experimentally and deviations of the measured frequencies from the theoretical values were about **4** percent. The transfer function given by Eq. **(35)** is non-minimum phase, as expected, exhibiting a positive zero at **35.683.**

Using the identification procedure described earlier, the parameters of the motor model (Eq. **(14))** were determined as: J = **0.005529** lb in. s^2, V = **0.01216** lb in./rad./s, K = **2.184** lb in./amp and CF/K = **0.132** amp.

6.3 Motor Position Control Loop. The motor position control loop is shown in Fig. **4.** The parameters of the controllers were designed (Rattan et al., **1988c)** to minimize the effects of the friction and to make the motor positioning as fast as possible. The sampling period was 3 ms. The response of the motor position when a step input of ±0.4 rad was applied as references θ_{mr} to the motor is shown in Fig. **11.** In this experiment, the tip of the arm was kept fixed in the zero angle position. There was a significant coupling torque between the motor and the beam (a beam deflection of **0.2** rad). The settling time was about 50 ms. This is fast as compared to the first natural frequency of the beam, but is not much faster as compared to the second. However, we will assume that the transfer function of the inner loop is 1 and we will show that good results are achieved with our method even in this case.

6.4 Tip Position Control Loop

6.4.1 Trajectory Design. The transfer function of the beam is non-minimum phase. Thus, according to Subsection **4.1.** we choose a quasi-parabolic profile. Acceleration and second derivative of the acceleration are chosen taking into account the mechanical constraints (maximum allowable deflection of the beam). These are: acceleration = **7875** rad/s^2, and 2nd derivative of acceleration = **8648.646** rad/s^4. In this case, using **(18),** a filter can be obtained as

$$G_{ff}(s)\hat{G}_n(s) = (1+0.0561s+0.00157s^2)\frac{35.683}{35.683}\frac{-s}{s} \quad (36)$$

Figure **12** shows the ideal quasi-parabolic trajectory $P_p(s)$ that drives the tip from **−0.1** rad to **0.1** rad, and the optimized reference trajectory $\theta_{nr}(t)$ resulting from passing P_p through filter **(36).**

6.4.2 Feedforward Term. The feedforward term can be obtained using expression **(19)** (expressed as a function of the payload m_2) as

$$\hat{G}_n(s) = (0.12136m_2s^4 + (176.6032m_2 + 2.6791)s^2 + 852.81575)\frac{1+0.0561s+0.00157s^2}{0.67(s+35.683)^2} \quad (37)$$

m_2 appears only in the first factor. This feedforward term may be easily tuned as a function of the payload using the scheme shown in Fig. **13.** This scheme implements expression **(37)** in such a way that the parameter to be tuned only effects the gains of three signals that are known before the motion (reference trajectory and its second and fourth derivatives). The dynamic component of the filter shown in Fig. **13,** which requires most of the computations of the feedforward term, is independent of the payload value. Substituting m_2 = **0.12136** lb for our beam, we get

$$\hat{G}_n(s) = (s^4+1637.1s^2+57903.3)\frac{1+0.0561s+0.001571s^2}{45.5(s+35.683)^2} \quad (38)$$

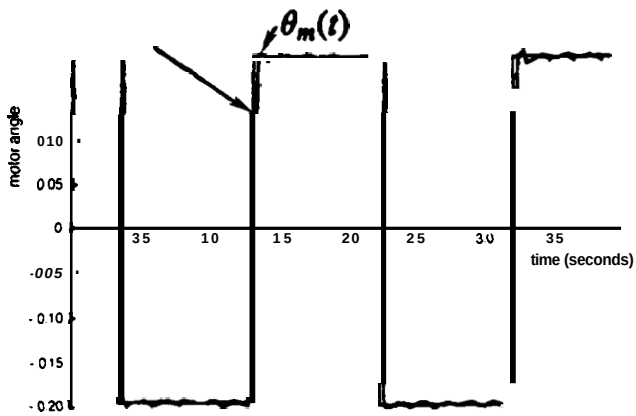

Fig. 11 Experimental response of the motor position control loop to step references

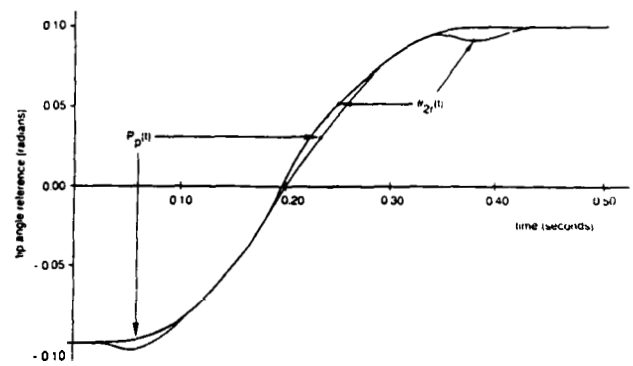

Fig. 12 Nominal trajectory P_p and optimum realizable reference trajectory θ_{2r}

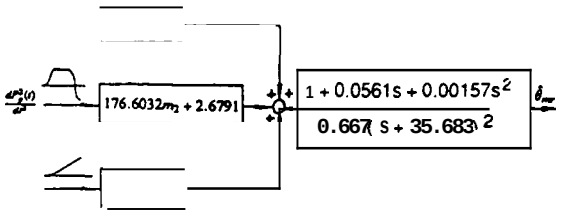

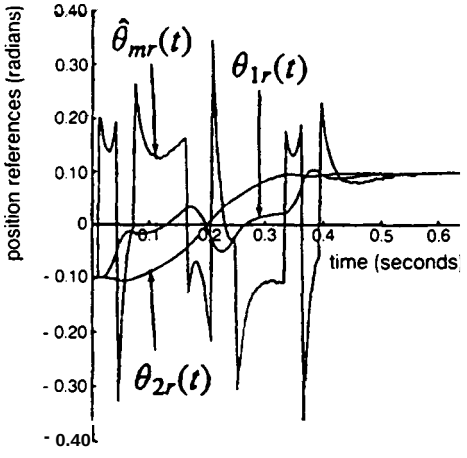

Fig. 14 Implementation of the feedforward *term*

6.4.3 Feedback *Controller.* We first need to calculate $\Upsilon(s)$ which gives the references for the measured variables. Using (23), we get

$$\Upsilon(s) = \begin{bmatrix} \dfrac{-98.88m_2s^2 + 1273.3}{s^2 - 1273.3} \\ 1 \end{bmatrix} = \begin{bmatrix} \dfrac{12s^2 + 1273.3}{s^2 + 1273.3} \\ 1 \end{bmatrix} \quad (39)$$

The first element of Υ is a function of the payload and may be tuned in the same way as the feedforward term. Figure 14 shows the plots of the references $\theta_1(t)$, $\theta_2(t)$ and $\theta_m(t)$ (feedforward term). In order to get the feedback controller, we chose a cost function (20) of the form: $Q_1 = \text{diag}(1, 2, 0, 0)$. $Q_2 = 1$, where we weighted the tip position twice the middle mass and motor positions. The optimum controller that minimizes the cost function (20) is given by

$$\Lambda = (0.4428 \quad 0.5572 \quad 0.0534 \quad 0.1828). \quad (40)$$

This places the closed-loop poles at $-3.79 \pm j7.375$, and $-6.61 \pm j40.506$. The closed-loop frequencies are of the same order of magnitude as the open-loop frequencies of the beam, but the oscillations are substantially damped. This closed-loop behavior is experienced only when perturbations are present in the arm. If there were no perturbations, the feedforward term alone (without the feedback loop) would produce a motion completely free of oscillation. Because of the limited calculation capability of our computer, the feedback loop is implemented with a sampling period of 6 ms (twice that of the motor control loop). Figure 15 shows the response of the tip to reference trajectory. The reference trajectories of the middle mass and the tip along with the response of the middle mass are shown in Fig. 16. Figure 17 compares the response of the motor to the responses of the middle mass and tip.

The fourth order parabola reaches the target position in 0.36 s. This is the fastest motion that can be achieved for this arm without producing deflections in the structure beyond its mechanical limit. Figure 15 shows that the tip reaches this position with an error of less than 2 percent in 0.4 s. It can be seen

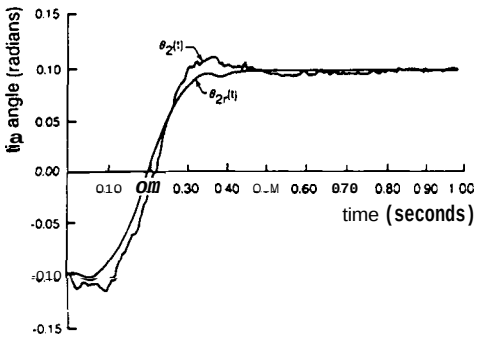

Fig. 15 Reference trajectory and experimental response of the tip

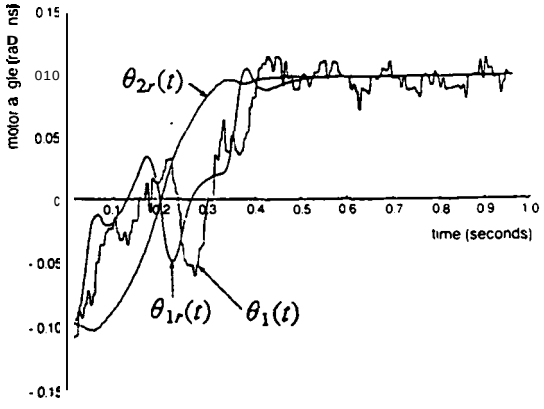

Fig. 16 Reference trajectory and experimental response of the middle mass

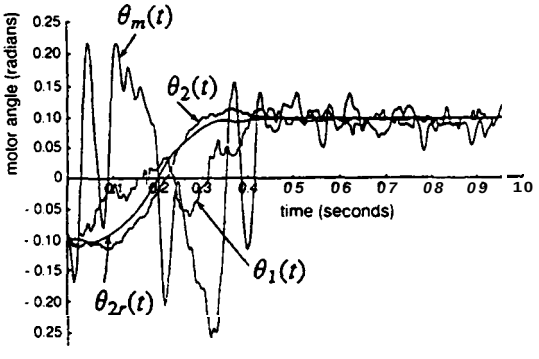

Fig. 17 Comparison of the responses of the motor, middle mass, and tip

that fast and accurate motions are achieved for this arm. Tracking errors in Fig. 15 are significantly smaller when the trajectory is slower. Notice the high level of noise of the camera measurements θ_1 and θ_2.

Figure 18 shows the simulation results of the tip response with and without the feedforward term. It can be seen from this figure that the use of the feedforward term removes the steady-state error which is otherwise noticeable. This is because of the low gains of the feedback controller. Note also that the transfer function between the motor and tip positions is of type zero whereas the transfer function between the motor current and the tip position is of type one or two. In comparing the systems with and without the feedforward term, it can be seen from this figure that when the feedforward term is active, there are no oscillations in the tip position which significantly reduces the settling time as compared to system without feedforward term.

7 Conclusions

Modeling, identification and control of single-link flexible

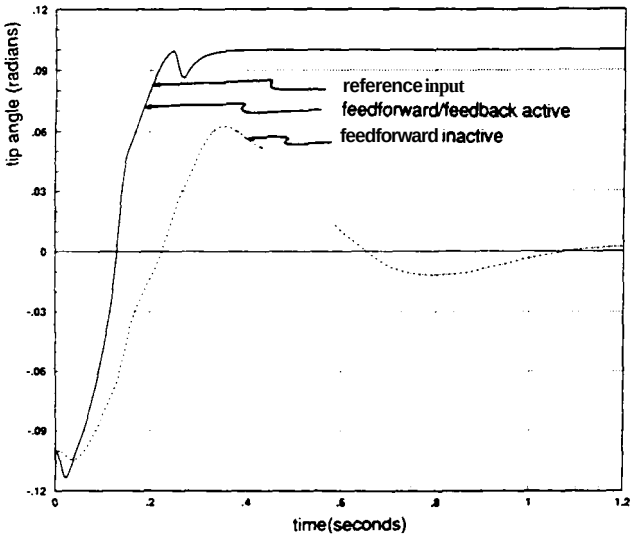

Fig. 18 Tip responses with and without the *feedforward* term

arms with lumped masses is studied in this paper. Most of the flexible arms have their mass distributed along the structure. But there are some applications in which a model using lumped masses may be useful. A typical example is the case of a lightweight flexible arm carrying a heavy load. Here, only one vibrational mode is normally important allowing an approximate modeling by a massless beam with a mass attached to the tip. Another reason to study flexible arms with lumped masses is that some properties and control methods for these systems may be extended to the distributed mass case. Techniques described in this paper refer to the following three aspects of flexible arms: modeling, identification, and control. In the case of modeling, the division of the arm model into motor and beam submodels is general, but the modeling of the beam submodel is specific to lumped mass flexible arms. The identification technique described in Section 5 *can* be applied to both lumped and distributed-mass flexible arms. The result is a dynamic model of the form (24) and (25). Provided that the model of a flexible arm is expressed in the form given by Eqs. (24) and *(25).* the control scheme described in Section 4 is general and may be applied to any flexible arm.

A method of modeling these systems has been presented in Section 2. In order to deal with nonlinear Coulomb friction, two submodels have been defined, one that describes the behavior of the motor (includes friction nonlinearities), and another linear submodel that describes the mechanical behavior of the beam. Both submodels are coupled by the torque at the base of the beam. In order to make the model more general, perturbations in the tip, represented by a torque and a force, have been considered. These perturbations allow us to consider the effects of friction in the tip in the model, changes in the carried load, or reaction forces produced by the next joint in the case of a multiple-link flexible arm. Although not used in this paper, some properties have been deduced from these dynamic models in Section 3. The most interesting one is the ***Separation Property*** that defines the influence of the masses of the beam in the model. It permits representing the product of the mass *i* and its angular acceleration by a linear combination of the deflections of the beam at the points where the masses are located. This linear combination depends only on the geometry of the beam.

A control scheme is proposed that minimizes the effects of the friction in the joints. This control scheme is composed of two feedback nested loops, an inner loop to control the motor position and an outer loop to control the tip position. Tip position control loop is designed in this paper. The design of the inner loop (motor position) was presented in previous papers (Rattan et al., 1988a, 1988b, 1988c). The control scheme for the tip position has been developed from our model and its properties. The controller for the tip position control loop is composed of feedforward and feedback terms. Nominal trajectory and feedforward term are designed taking into account whether the system is minimum or non-minimum phase. A method to optimize the feedforward term was presented for the non-minimum phase case. Other feedforward control methods for flexible arms are based on generating a current (torque) to drive the arm (Meckl and Seering, 1988 and Farrenkopf, 1979). But, they cannot be used when the joint has a significant Coulomb friction. Our method is based on generating a motor position command. This simplifies significantly the command signal, allowing it to be generated in real-time. Our control scheme is robust to nonlinear friction in the joint and is taken care of by the inside loop. Another important advantage not exhibited by other methods is that this command profile may be easily modified as a function of the actual payload, making it suitable for real-time adaptive control. This is a consequence of the ***Zeros invariancy property.***

A feedback controller was designed using an optimization criterion. Effects of changes in the tip's mass were also studied. Modeling and control methods have been generalized in Section 5 to the distributed-mass flexible arm case. Therefore, the results presented in this paper are valid for all single-link flexible arms. Controllers designed here are simpler than the ones obtained using other methods. This is because of the assumption that the inner loop makes the motor respond to position commands without any delay and by using more sensing than in other methods. Reconstruction of nonmeasured states from only motor and tip measurements, using filters or observers, is avoided. Consequently, little computational effort is needed and the measured signals *can* be sampled at a very high rate improving the performances of the computer controlled arm (Franklin and Powell, 1980). A limitation of our method is the necessity of achieving a motor response faster than the vibrational modes considered in the model of the beam.

Finally, some experimental results have been presented. Modeling and control methods have been applied to a lumped two-mass flexible arm that we built in our laboratory. Results that the limitation mentioned in the above paragraph may be relaxed in many cases. The control system also proved to be quite insensitive to noise in the measurements, and to errors in modeling (about 5 percent in the estimation of natural frequencies). The arm used in this paper is very flexible. This means that in order to quickly remove small errors in the tip position, relatively large deflections were needed, and the motor had to experience large motions.

Acknowledgments

The research described in this paper was performed at the Robotics Institute, Carnegie-Mellon University, Pittsburgh, Pennsylvania. The authors are grateful to the associate editor, Dr. Suhada Jayasuriya, and the reviewers for their encouraging and helpful comments.

References

Book. W. J., 1979, "Analysis of Massless Elastic Chains with Servo Controlled Joints." ASME JOURNAL OF DYNAMIC SYSTEMS, MEASUREMENT, AND CONTROL. Vol. 101.

Cannon, R. H., and Schmitz, E., 1985, "Precise Control of Flexible Manipulators," *Robotics Research.*

Craig, J. J., 1966, *Introduction to Robotics: Mechanics and Control,* Addison-Wesley, Reading. MA.

Farrenkopf, R. L. 1979, "Optimal Open-Loop Maneuver Profiles for Flexible Spacecraft," *Journal of Guidance and Control.* Vol. 2, No. 6.

Feliu, V.. Rattan. K. S.. and Brown, H. B., 1989, "A New Approach to Control Single-Link Flexible Arms. Part III: Control of the Tip Position in the

Presence of Joint Friction," Technical Report #CMU-RI-TR-89-15, Robotics Institute, Pittsburgh, Pennsylvania.

Feliu. V.. Rattan, K. S.. and Brown, H. B., 1988, "Model Identification of a Single-Link Flexible Manipulator in the Presence of Friction,'' ***Proc. of the 19th ISA Annual Modeling and Simulation Conference,*** Pittsburgh, PA.

Feliu, **V.,** Brown, H. B., and Rattan, Kuldip **S.,** 1989, "Design and Control of a Two-Dcgree-of-Freedom Flexible Arm," Technical Report #CMU-RI-TR-89-21, Robotics Institute. Pittsburgh, PA.

Franklin, G. F., and Powell. J. D., 1980, *Digital Control of Dynamics Systems*, Addison-Wesley. Reading, MA.

Gupta. **S.** C.. and Hasdorff. L.. 1970, *Fundamentals of Automatic Control.* John Wiley & **Sons,** Inc.

Kotnick, T., Yurkovich, **S..** and Ozguner, U.. 1988. "Acceleration Feedback for Control of a Flexible Manipulator **Arm,"** ***Journal of Robotic System,*** Vol. **5**, **No. 3.**

Kuo, B. C., 1982, *Automatic Control Systems,* Prentice-Hall.

Lancaster, **P..** and Tismenetsky, M., 1985, ***The Theory of Matrices, Second Edition with Applications***, Academic Press.

Lee. E. B.. and Markus. L., 1986, ***Foundations of Optimal Control Theory,*** Krieger Publishing Co.. Florida.

Low. K. H., 1987. "A Systematic Formulation of Dynamic Equations for Robots Manipulators with Elastic Links," ***Journal of Robotic System,*** Vol. **4, No.** 3.

Matsuno. F., Fukushima, **S..** and coworkers, 1987. "Feedback Control of **a** Flexible Manipulator with a Parallel Drive Mechanism," ***International Journal of Robotics Research,*** **Vol. 6, No. 4.**

Meckl, P. H.. and Seering, W. P.. 1988. "Reducing Residual Vibration in Systems with Uncertain Resonances," ***IEEE Control Systems Magazine,*** Vol. **8, No. 2.**

Rattan, K. **S..** Feliu. **V..** and Brown, H. B., 1988a, "A Robust Control Scheme for Flexible Arms with Friction in the Joints,'' ***Proc. of the Second Annual Workshop on Space, Operation. Automation and Robotics.*** Dayton, Ohio.

Rattan, K. **S.,** Feliu, V.. and Brown, **H.** B.. 1988b, "Experiments to Control Single-Link Lightweight Flexible Manipulator with One Vibrational Mode,'' ***Proc. of the ISA International Conference on Robotics and Expect System,*** Houston, Texas.

Rattan, **K. S..** Feliu, V.. and Brown, **H.** B.. 1988c, "Identificationand Control of a Single-Link Flexible Manipulator." ***Proc. of the 27 IEEE Conference on Decision and Control,*** Austin, **Texas.**

Truckenbrodt. A.. 1979. ''Dynamics and Control Methods for Moving Flexible Structures and Their Application to Industrial Robots," ***Proc. of the 5th World Congress on Theory of Machines and Mechanisms.***